5-2024

Suppressing Reactive Oxygen Species via Application of Antioxidant Supramolecular Polymers

Zacchaeus Wallace

Suppressing Reactive Oxygen Species via Application of Antioxidant Supramolecular Polymers

by

Zacchaeus Wallace

A Thesis
Submitted to the Honors College of
The University of Southern Mississippi
in Partial Fulfillment
of Honors Requirements

May 2024

Approved by:

Tristan Clemons, Ph.D., Thesis Advisor,
School of Polymer Science and Engineering

Derek Patton, Ph.D., Director,
School of Polymer Science and Engineering

Joyce Inman Ph.D., Dean
Honors College

ABSTRACT

Cardiovascular diseases along with various other disease conditions are characterized by an upregulation in reactive oxygen species (ROS), which can overwhelm homeostatic processes in the body, resulting in cellular apoptosis and severe oxidative damage. The lack of clinically approved treatments to regulate or alleviate this elevated ROS presence underscores the need for novel therapeutic strategies. While antioxidants promote cell rescue through ROS scavenging, their clinical translation is impeded by insufficient bioavailable concentrations at the source of injury. The opportunity to apply antioxidant supramolecular polymers of peptide amphiphiles (PAs) is an exciting prospect of research to combat corresponding issues. For this work, a PA monomer was designed and synthesized to incorporate antioxidant activity, modelled off the potent and natural antioxidant, glutathione. PAs were characterized for molecular weight and purity using liquid chromatography mass spectrometry. The supramolecular polymerization of these PAs was assessed by a Nile Red assay to determine the critical aggregation concentration of the PA monomers, circular dichroism to assess internal ordering of the PA molecules upon assembly, and transmission electron microscopy to assess nanofiber morphology. The antioxidant capabilities were probed using a 2,2-diphenyl-1-picrylhydrazyl assay. Finally, the cellular viability and efficacy in ROS mitigation of the antioxidant supramolecular polymers assessed in the *in vitro* setting. Taken together, these results provide exciting proof-of-principle support of antioxidant supramolecular polymers as a potential new therapeutic approach to target the damaging effects of ROS in disease and injury.

Keywords: Reactive oxygen species, supramolecular polymers, antioxidant therapies, peptide amphiphiles, biomaterial, glutathione.

DEDICATION

I dedicate this work to all of those important to my life. To God for all the blessings I've been bestowed. To my mother, Dr. Kedra Wallace, my father, Zacchaeus C. Wallace, and my brothers, Nathanael and Jonathan Wallace. To my grandparents, Grace and Bennie Wallace and Connie and Robert Martin. To the rest of my family. To my friends who supported me throughout my college journey. To my partner, Azariah Russ and my best friends: Bryan Nevills and Hunter Smith for their constant support and love. To my first student organization, the Men of Excellence, for contributing to my growth in all aspects of life. To the Office of Inclusion and Multicultural Engagement, the Mu Xi Chapter of Alpha Phi Alpha Fraternity Inc., the Student Government Association, EagleTHON, and the Honors College. To my advisors, Jaborius Ball, Hannah Scott Back, Carl Thomas, and Tristan Clemons, for their support, advice, and trust. Finally, to the School of Polymer Science and Engineering and the 2024 Class.

ACKNOWLEDGMENTS

I would like to acknowledge Dr. Sabine Heinhorst and Dr. Joyce Inman, the individuals who played the most impactful role in my choosing of the University of Southern Mississippi (USM) four years ago. Thank you for all the advice and editorial expertise you have given throughout my undergraduate career. I would like to acknowledge Dr. Broadhead for her academic advising to put me in a great position to succeed as an honors student and polymer scientist and engineer. I would like to acknowledge the IDEA Network of Biomedical Research Excellence (INBRE) for access to cell culture facilities and characterization instrumentation. I would also like to acknowledge the funding agencies that supported my honors research including the USM Drapeau Foundation through an Eagle SPUR award, and the National Institutes of Health (NIH) National Institute of Biomedical Imaging and Bioengineering through award (R21EB033533). I would like to acknowledge the undergraduates, graduate students, and team members of the Clemons Lab. A special thanks to Charles “Mac” McCormick, my fellow Clemons Lab senior and friend who has taken every class with me as well as served as a member on our Senior Capstone team. I want to thank my graduate student mentor, Penelope Jankoski, for the mentorship and patience as this research has progressed since my joining in the lab. Thank you for the flexibility, encouragement, and positivity through my busy schedule. Finally, I would like to acknowledge my thesis advisor and research mentor, Dr. Tristan Clemons. Thank you for accepting me into your research lab, for the tough love, for the time spent on me to ensure that I achieved the goals that I wanted, and for the opportunity presented for me to grow as an individual, professional, and competitor. Most of all, thank you for believing in me.

TABLE OF CONTENTS

LIST OF ILLUSTRATIONS

LIST OF ABBREVIATIONS

CAC	Critical Aggregation Concentration
CD	Circular Dichroism
CVD	Cardiovascular Disease
DPPH	2,2-diphenyl-1-picrylhydrazyl
DMF	Dimethylformamide
DMSO	Dimethyl Sulfoxide
E_3	Peptide amphiphile with peptide sequence: C_{16}-VVVAAAEEE
EDTA	Ethylenediaminetetraacetic Acid
ESI-MS	Electrospray Ionization Mass Spectrometry
FMOC	Fluorenylmethoxycarbonyl
GSH	Glutathione
HPLC	High-Performance Liquid Chromatography
I/R	Ischemia-Reperfusion
LDH	Lactate Dehydrogenase
MALDI-TOF	Matrix-Assisted Laser Desorption/Ionization Time-of-Flight
PA	Peptide Amphiphile
ROS	Reactive Oxygen Species
SPPS	Solid Phase Peptide Synthesis
TBHP	Tertbutyl Hydroperoxide
TEM	Transmission Electron Microscopy
TFA	Trifluoroacetic Acid

CHAPTER I: INTRODUCTION

1.1 Cardiovascular Disease

Cardiovascular disease (CVD) is referred to as a group of disorders affecting the heart and blood vessels.[1] At over 20.1 million deaths annually, cardiovascular disease is the world's leading cause of death.[2] Additionally, Mississippi consistently stands out among the Southern states with one of the highest prevalence rates of CVD. Based on statistics from the past two decades, mortality attributed to CVD comprises over a third of all deaths recorded in Mississippi underscoring the urgency of targeted therapies and public health strategies.[2] The occurrence of and growth in CVD stems from the interconnections of aging, unhealthy lifestyle habits, tobacco and alcohol consumption, and genetics leading to risk factors such as obesity, diabetes, high blood pressure, and other disorders.[1] The increase in urbanization and industrialization further exacerbates the prevalence of cardiovascular disease in a trend known as the "inverse social gradient".[3] This trend is evident as many countries have acquired and will continue to acquire access to improved medical care leading to an extended life expectancy which correlates to the development of CVD. The high mortality rate and trend of increase highlights the need for research that is tailored to reduce the rate of CVD and improve the corresponding treatment.

1.2 Oxidative Damage in Cardiovascular Disease

A hallmark of this condition, as well as many other pathologies, is the upregulation of reactive oxygen species (ROS). ROS are highly transient molecules, such as hydrogen peroxide, hydroxyl radicals, singlet oxygen, and superoxide species. In the healthy state, ROS production is controlled and regulated, contributing to several processes including redox signaling, immune defenses, and baseline homeostatic mechanisms. In the disease

state, the increase of ROS overwhelms homeostatic processes in the body resulting in cellular apoptosis and severe oxidative damage to surrounding cells, thereby causing further damage.[4] Mitochondria are particularly sensitive to the effects of damaging ROS, and damage to the mitochondria further upregulates ROS production leading to cell death through necrotic and apoptotic mechanisms via redox signaling.[5,6,7] Redox signaling is the body's system involving the balance of oxidative stress and antioxidant defenses on a cellular level. Kinases are enzymes that, when activated by ROS, initiate apoptotic processes. In ROS upregulation, the kinases, c-Jun N-terminal kinase (JNK), extracellular signal-regulated kinase ½ (Erk1/2), p38 mitogen-activated protein kinase (p38 MAPK), and Ca/calmodulin-dependent kinase II (CAMKII) contribute to apoptosis through their triggering of apoptotic proteins (**Figure 1**).[8]

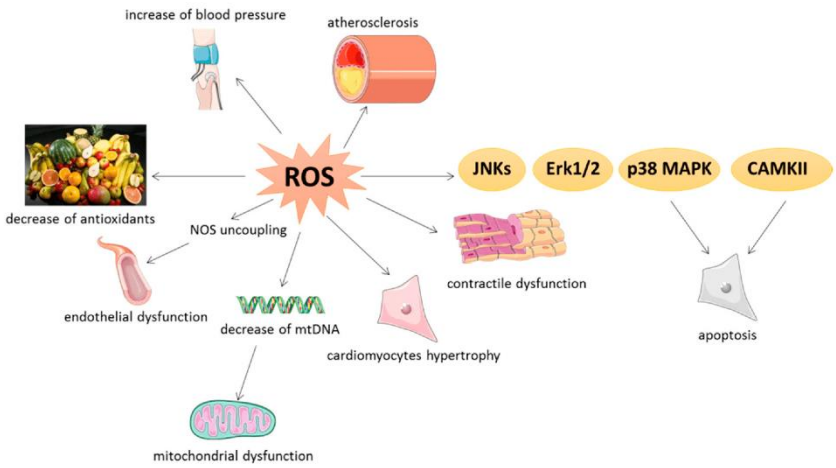

Figure 1. *Role of oxidative stress in cardiovascular tissue attributed to ROS upregulation.*[8]

ROS are capable of initiating lipid peroxidation, a process that results in the degradation of lipids in cell membranes. This oxidative damage compromises membrane integrity, disrupting cellular signaling and transport processes. Additionally, lipid peroxidation

generates reactive byproducts that further propagate oxidative stress and inflammation, amplifying cellular damage.

Cardiac ischemia-reperfusion (I/R) injuries occur from an interruption in the heart's blood supply.[9] The ischemic process is described as the process when cells become damaged due to the lack of oxygen supplied to the heart. Reperfusion is the restoration in blood flow and can result in further injury as ROS is released due to the sudden surge in oxygen resulting in oxidative stress to vulnerable tissues. ROS overproduction impairs mitochondrial function, and elevates oxidative stress, inflammation, and apoptosis.[10] Although the body's protective mechanisms mitigate the impact of cardiac I/R, the sharp increase in ROS overcomes these protective strategies, hence the need for better therapeutic strategies.[11]

1.3 Current Antioxidant Approaches

In the body, antioxidants play a pivotal role in counteracting oxidative stress by neutralizing ROS. Antioxidant therapies explored for CVD include nutritional supplements, experimental antioxidant compounds, microRNAs, and therapeutic nanoparticles.[12] Dietary antioxidants such as vitamins A, C, E, and omega-3 are acquired through food intake and have demonstrated efficacy, when at a sufficient concentration, in alleviating complications associated with CVD by quenching ROS.[12] These vitamins exert their influence by modulating and regulating cell proliferation and redox pathways. Experimental compounds found in clinical drugs activate endogenous antioxidant defense systems such as NRF2, or though inhibiting oxidative stress formation. Furthermore, the development of nanoparticles designed to target ischemia/reperfusion (I/R) injury has exhibited anti-inflammatory and anti-apoptotic activities as they can be functionalized to

selectively accumulate within ischemic tissues.[12] With increasing capabilities to incorporate antioxidant therapies, nanoparticles showcase a promising avenue in antioxidant-based interventions for cardiovascular health.[13,14]

The quenching nature of antioxidants makes them as an ideal approach in the development of oxidative therapies. However, antioxidant therapies have translated poorly to the clinic for varying reasons.[15] The challenges within the above therapeutic approaches arise from the complex signaling pathways inherent in cellular processes and the struggle to localize antioxidants at the site of injury with a persistence time long enough to effectively mitigate ROS following acute trauma. The efficacy of antioxidants in neutralizing ROS depends on their concentration and their ability to reach the specific sites of oxidative stress. The notable limitation of inadequate localization is actively under investigation in this scope of research, exploring novel materials to enhance therapeutic effectiveness in cardiovascular disease. Continued advancements in these therapeutic strategies are a subject of constant scrutiny, driven by the potential benefits of surpassing existing limitations and refining targeted practices for improved outcomes in the management of oxidative stress.

1.4 Peptide Amphiphile Supramolecular Polymers

Supramolecular polymers offer appealing material options for use in regenerative scaffolds. This is because signaling within the extracellular matrix relies heavily on proteins. Short peptide epitopes can mimic the function of these proteins, enhancing the versatility and effectiveness of these materials.[15, 16, 17] The investigation into regenerative applications entails strategically integrating antioxidant properties with supramolecular polymers.

Supramolecular chemistry emerged in the late 1970s as a promising field providing several ideal characteristics in controllability and self-assembly to form well-defined structures.[16] As the term "supramolecular" suggests, the molecules self-assemble driven by noncovalent interactions into various nano and macroscale structures (**Figure 2).** [17] Supramolecular chemistry focuses on the weaker, non-covalent interactions in molecules including hydrogen bonding and electrostatic interactions. These non-covalent interactions are similar to those seen in biological systems highlighting its relevance in biomedical applications. Supramolecular systems exhibit the property of self-assembly which allows for the formation of complex structures that can be engineered to react in various biological instances advantageous in biomedical scaffolds and engineering devices.[18] These properties enable the incorporation of targeting ligands tailored to interact with specific receptors or biomolecules on target cells. This specificity is particularly valuable in the treatment of complex diseases where conventional therapies may lack selectivity. Peptide amphiphiles are an exciting class of supramolecular polymers that are bioactive, biocompatible, and biodegradable.[17] They are comprised of amino acid repeat units which form the peptide head and a hydrophobic tail, where the peptide sequence dictates nanostructure formation and can be designed to interface with the body (**Figure 3.)**. The hydrocarbon tail collapses in an aqueous environment and strong intermolecular bonding between amino acids drive the formation of nanostructure

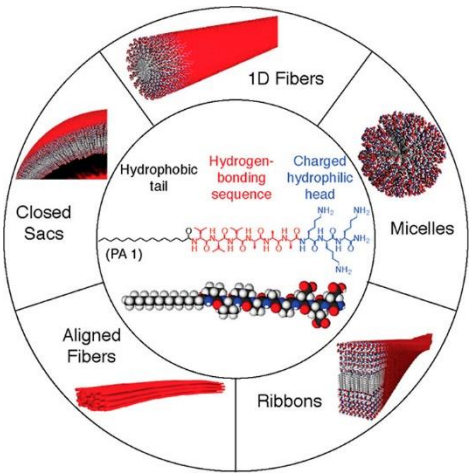

Figure 2. *Supramolecular structures derived from peptide amphiphiles.*[17]

into a fibril like structure. By altering the amino acid sequence, different nanostructures can be obtained. Specifically, the hydrophilic head is typically a peptide sequence of amino acids that form the polar region of the polymer. This sequence is designed to guide the biological capabilities and interactions of the PA. The hydrophobic region of the PA yields the self-assembly properties. Self-assembly is often achieved through the conjugation of a fatty acid, providing a lipid tail. The bioactive sequence can provide cues to the biological environment or act as a therapeutic. The arrangement of the PA components leads to its ability to form various structures such as micelles or nanofibers. These PA supramolecular polymers are an exciting class of biomaterials for tissue regeneration applications due to their tissue targeting capabilities and capacity to mimic the organization of the extracellular matrix with their filamentous structure.[16] Further, as PA monomers are held together by non-covalent interactions, they provide a facile method for combining both polymeric and antioxidant properties.

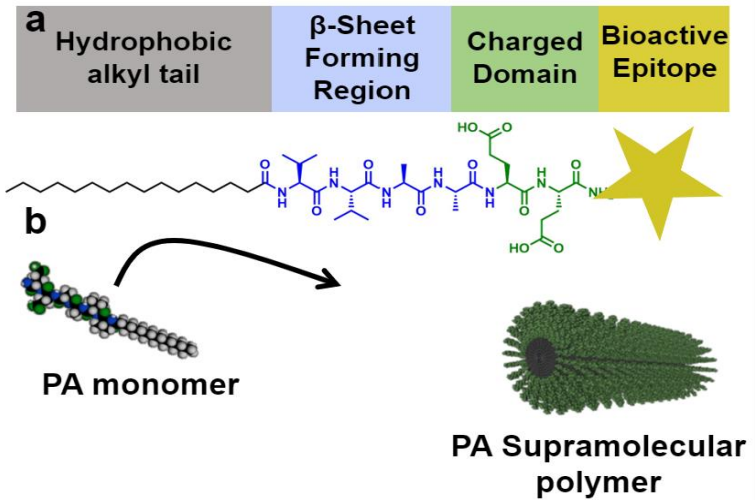

Figure 3. *a) The four structural components of peptide amphiphiles. b) Self-assembly of monomers into supramolecular polymer.*

Crucial to this study, the diluent PA, C_{16}-VVVAAAEEE (E_3) is a well-established sequence, with demonstrated fiber forming capabilities and rapid self-assembly.[15] Glutathione (GSH), a potent and natural antioxidant, is one of the main components of

our natural defense system against ROS in most living cells. It is a tripeptide composed of the amino acids, glycine, cysteine, and glutamic acid, primarily found intracellularly. Functions of GSH include antioxidant defense, detoxification of foreign chemical substances, regulation of cell cycle growth and death, cysteine storage, redox signaling, modulation of immune function, and wound healing mechanisms.[19,20] Due to these functions, GSH is an antioxidant of interest to be applied in antioxidant therapies.[21] GSH promote cell rescue by scavenging free radicals such as ROS and thereby protecting surrounding cells. Possible GSH applications are studied in this work to determine the biomedical capabilities of this antioxidant for suppressing the levels of ROS among disease conditions.

1.5 Statement of Research

Motivated by the lack of clinically approved therapies for the effects of ROS in cardiovascular disease, we aim to evaluate the synthesis and bioactive abilities of an antioxidant supramolecular polymer. Thus, the goal of this research project is to develop a biochemical strategy to mitigate the damaging effects of ROS upregulation and generate scaffolds for tissue regeneration at the site of disease, with the hope of developing materials to provide therapy in cardiac ischemia-reperfusion (I/R) injuries. For the purpose of this work, the self-assembly of peptide amphiphiles were designed to be combined with antioxidant properties. The novel synthesis of a glutathione peptide amphiphile coupling is hypothesized to show positive correlation with both fiber formation and bioactivity. Results of this investigation would lead to significant strides in the therapeutic knowledge and capabilities surrounding reactive oxygen species.

1.6 Techniques & Characterization

1.6.1 Solid Phase Peptide Synthesis

Solid Phase Peptide Synthesis (SPPS) is the most recent and practical method of peptide synthesis used for a wide range of commercial and pharmaceutical products. This technique consists of peptide assembly stepwise from its C-terminus using successive addition of the protected amino acids, where the growing peptide chain is tethered to a solid resin bead support. Each addition follows the steps of: cleavage of the N^{α}-protecting group and amino acid coupling with washing steps ensuring complete removal of cleavage agents and excess reagents, to ensure only a single addition each time, providing sequence control.[22,23,24] The described synthesis highlights the Fmoc protection process which is used for acid sensitive peptides with modified sidechains. This method is mild and versatile as it offers more synthetic peptide options compared to the alternative Boc protection process.[22] Commercial products and reagents are readily available, allowing for peptide synthesis to occur with ease.

1.6.2 High-Performance Liquid Chromatography (HPLC)

Chromatography is a common biophysical technique for separation, purification, and identification of components like peptides contained in a sample. High-Performance Liquid Chromatography (HPLC) consist of a column dedicated for molecular separation and pumps that deliver solvent at a controlled flow rate. HPLC is used for dissolved compounds and provides qualitative and quantitative analysis of the sample's components. The process of this chromatography technique consists of pump delivery of solvents and the sample to the column. The sample mixture, dissolved in a solvent known as the mobile phase, is injected into the column. As the mobile phase flows through the column under high pressure, the components of the sample interact differently based on

their chemical properties, such as polarity, size, and charge. This interaction leads to differential retention times for each component as they traverse the column resulting in peaks as shown in the chromatogram.

[25,26]

1.6.3 Mass Spectrometry

Mass spectrometry is a technique used to calculate molecular weight through the mass-to-charge ratio (m/z) measurements of molecules present in a sample. This technique provides both qualitative and quantitative information after ion conversion. Electrospray Ionization (ESI) makes use of electrical energy to transfer ions from solution phase into the gaseous phase. This transfer follows the stages of droplet formation, desolvation, and gas phase ion formation.[27] As a soft ionization method, ESI has improved sensitivity, accuracy, and complexity of analytical mixtures making it useful for monitoring target peptides and their complete sequence.[28] Additionally, Liquid Chromatography-MS is employed to assess composition further by coupling chromatogram peaks with their resulting mass spectrum.

1.6.4 Transmission Electron Microscopy (TEM)

Transmission Electron Microscopy (TEM) is a technique for the visualization of nanostructures formed by peptide amphiphiles. TEM implements electron beams which have wavelengths ~100,000x smaller than those of visible light when accelerated through a strong electromagnetic field. This capability allows the researcher to view the nanostructures of materials which lead to further understanding of structural connections. Opposed to traditional techniques, TEM provide valuable information pertaining to the morphology and defects present at the nanoscale level. The five key components of a

TEM are its high voltage system, vacuum system, microscope column, detectors, and control computers and software.[29,30] Together, these components make TEM essential in correlating structural information for peptide sequence and self-assembly. Samples are placed on a copper mesh grid and the electron beam is transmitted through the sample providing information on the nanostructure.

1.6.5 Circular Dichroism

Circular Dichroism (CD) is a spectroscopy method capable of measuring the self-assembly behavior of peptide amphiphiles and providing insight into the supramolecular organization in solution in both quantitative and qualitative manner. CD measures the difference in the absorption of left-handed and right-handed circularly polarized light stemming from varying factors. Signal intensity is directly related to molecular conformation, secondary structure content, and protein folding tendencies. Known characteristic CD spectra for varying secondary structures are compared to the signal intensity to determine what structuring is present in the given sample. The method allows for the rapid evaluation of the secondary structure, folding, and binding properties of proteins.[31] For this work, CD is used to qualitatively assess the internal ordering to ensure that the β-sheet region of the peptide amphiphile is present.

1.6.6 Nile Red Assay

The Nile Red assay is a technique used to assess the self-assembly and nanofiber formation of PAs by detecting changes in fluorescence intensity upon interaction with hydrophobic domains. In this study, we utilize the Nile Red assay to investigate the self-assembly behavior of PAs. Furthermore, by determining the critical aggregation concentration (CAC) using Nile Red, we highlight the threshold concentration at which

PAs transition to assembled states, offering valuable information for optimizing their self-assembly properties. This comprehensive approach combining the Nile Red assay and CAC determination allows for understanding of PA self-assembly behavior.

1.6.7 2,2-diphenyl-1-picrylhydrazyl (DPPH) Assay

2,2-diphenyl-1-picrylhydrazyl (DPPH) is a free radical-containing compound stabilized by the delocalization of its spare electron.[32] This free radical can be used to measure the antioxidant trapping capabilities of radical quenching compounds mixed with DPPH in solution. DPPH undergoes a distinct color change from purple with the radical to a clear yellow without the radical, allowing for quantification of antioxidant potential of molecules to be assessed via spectrophotometry. Hence through measuring absorbance representative of the DPPH radical at 517 nm following material addition, the antioxidant content and efficacy can be assessed. For this work, the DPPH assay is used to assess the scavenging properties of our antioxidant PAs.

1.6.8 *In Vitro* Assays

In vitro assays encompass techniques that are conducted outside of a living organism and study therapeutic potential. Evaluating biocompatibility and cytotoxicity through cell culture is crucial to understanding the therapeutic potential of synthesized peptide amphiphiles for future translation into clinical applications. The use of culturing cells allows for the demonstration of cell viability pre and post amphiphile treatment. The implementation of LDH and fluorescent imaging provides a comprehensive view of how cells are affected.

The Lactate Dehydrogenase assay is a cytotoxicity assay that assesses the damage done to the plasma membrane of a cell population. LDH is a stable enzyme found in the

cytosol of cells. Following cell death, it is released into the supernatant and reacts with the LDH kit substrate to produce formazan. Formazan produces a signal at 480nm, allowing its intensity to be read on a plate reader that provides a way to precisely measure LDH release. Measurement of this LDH release is an insightful method for detection of necrosis/cytotoxicity. Performed in a 96 well plate, this reaction can be read through a microplate reader. This assay is conducted in this research to determine the biocompatibility of the synthesized PAs.

CHAPTER II: EXPERIMENTAL

2.1 Materials

Solvents including dimethyl sulfoxide (DMSO), methanol, dimethylformamide (DMF), N,N'-diisopropylcarbodiimide (DIC) were obtained from Sigma-Aldrich unless otherwise specified. Nile red was purchased from Apex Bio, DPPH was purchased from the Cayman Chemical Company, tertbutyl-hydroperoxide (TBHP), LDH Cytotoxicity Assay, and Live/Dead Imaging kits were obtained from Thermofisher . Additionally, chemicals required for peptide synthesis were sourced from CEM to synthesize the peptide amphiphiles under study including Rink Amide resin, Oxyma activator base, and all amino acids. These chemicals were of analytical grade and were used according to established protocols for peptide synthesis. Remaining chemicals were purchased at the highest available purity from Thermofisher Scientific or Sigma-Aldrich. All materials were stored and handled in accordance with manufacturer instructions and laboratory safety guidelines to ensure the accuracy and reproducibility of experimental results.

2.2 Solid Phase Peptide Synthesis and Purification

Solid Phase Peptide Synthesis was conducted using the Liberty Blue Microwave Peptide Synthesizer paired with the CEM Prodigy Peptide Purification System. Once amino acid reagents were properly dissolved in DMF at 0.2 M according to the desired method, peptides were synthesized on instrument **(Figure 4)**. Following the final Fmoc deprotection, a 90° C microwave coupling was applied to couple palmitic acid (in DMF, 0.2 M) to provide the hydrocarbon tail.

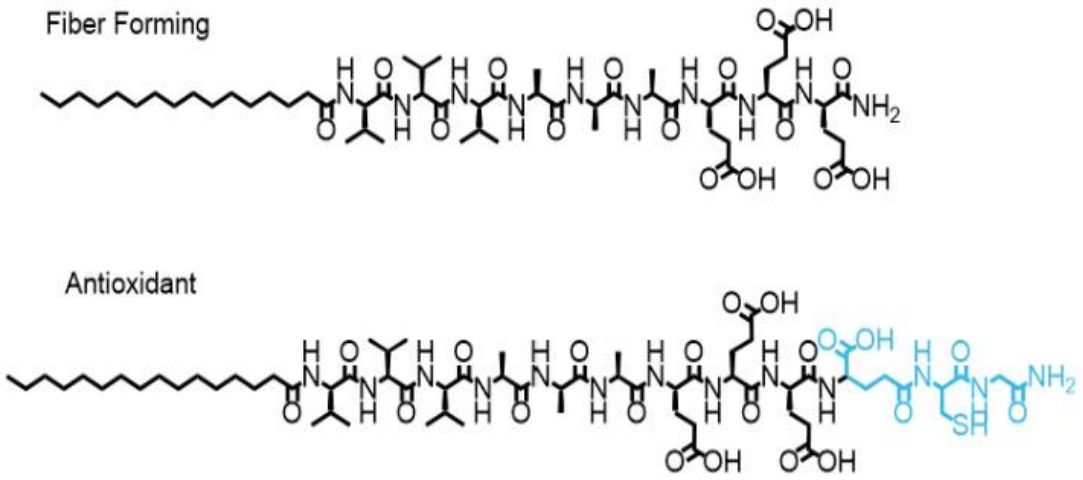

Figure 4. *Target peptide sequences indicative of supramolecular assembly.*

A glass peptide synthesis vessel containing peptide resin beads in DMF solution was clamped in a fume hood to further complete synthesis by using an acidic solution to knock the resin beads completely off the prepared peptide. DMF was blown off the solution with nitrogen to prepare Fmoc resin deprotection. A cleavage solution composed of trifluoroacetic acid (TFA) (18.5 mL), triisopropyl silane (TIPS) (0.5 mL), ethylenediaminetetraacetic acid (EDTA) (0.5 mL), and water (0.5 mL). This solution was added to the vessel containing the resin-bound PAs. This peptide and deprotection solution was then placed on a Burrell Wrist Action Shaker Model 75 for four hours of consistent shaking. Subsequently, the vessel solvent was dripped into four 50 mL Falcon Tubes filled with cold ether. This resulted in the precipitation of the PAs, typically as white wispy solids. The tubes containing the precipitate were placed in a freezer for 10 minutes to aid in the precipitation process. The solution was then centrifuged at 5000 RPMs for two minutes total with a break at one minute to vent for pressure. The ether was decanted off and the solid precipitate was collected. In cases where the PAs failed to

pelletize, more ether was added and left in the freezer overnight and the process was repeated. Peptides were left to dry overnight and dissolved for purification in 10% acetonitrile, 90% water with .1% NH4OH. Crude peptides were then purified using preparative reverse-phase HPLC with a water-acetonitrile (each containing 0.1% v\v NH4OH) gradient. Efficient runs included system purging at 20 mL/min, insertion into the column, and collection after 26 minutes when indicative peaks form. The mass and identity were determined using negative-ion mode MALDI-TOF. Fractions were rotovapped to remove acetonitrile and lyophilized to produce final powdered peptide. The powdered peptide is dissolved in deionized water to be 10 mM and treated with sodium hydroxide to reach a neutral pH of ~7.4-8. Once at an ideal pH, the peptide is lyophilized. This base-adjusted, dried, synthesized peptide was used in downstream experiments.

2.3 Transmission Electron Microscopy

TEM samples were prepared by adding 5 μL of peptide amphiphile samples (0.5 mM) onto 200 mesh carbon coated copper TEM grids for 3 minutes before remaining liquid was wicked with a Kimwipe. The staining agent, uranyl acetate, was placed dropwise on the grid and wicked away to serve as a negative stain for microscopy. Finally, 5 μL of water was placed on the grid and wicked away to wash excess uranyl acetate. Samples air dried and were imaged on a Delong Low Voltage Electron Microscope 25 (LVEM 25).

2.4 Circular Dichroism

Peptide amphiphiles are prepared at concentrations of 125, 250, and 500 μM and loaded into a UV-vis quartz cuvette at a volume of 250 μL respectively. Different concentrations are probed to ensure there is no effect of concentration on self-assembly

above the CAC. The cuvette is inserted into the spectrophotometer, following the manufacturer's instructions. Spectra are collected over a wavelength range of 190-300 nm with a bandwidth of 1 nm and a scanning speed of 100 nm/min. To ensure accuracy, each sample is analyzed three times, and averaged after applying baseline corrections. To eliminate the effects of Linear Dichroism, the cuvette is flipped, and three additional runs were acquired to be averaged with the initial runs. The resulting spectra are processed to generate a graphical representation of the data.

2.5 Nile Red Assay

The Nile Red assay starts with a 10 mM Nile Red stock (3.1837 mg/mL) in DMSO solution. This stock is then diluted down to 100 μM (0.5 μL stock added to 499.5 μL DI water). 10 mM of the PA stock is diluted to a lower concentration of 1 mM which is further diluted into 12 samples at 400 μL each (0, 0.1, 1, 2, 5, 10, 20, 25, 50, 100, 250, 500 μM). Samples used in this assay included E_3, glutathione antioxidant, and glutathione PA.

In a 96 well plate, 90 μL of each sample are added in triplicate and mixed adequately with 10 μL of the Nile Red stock. The well plate is then set in the dark to incubate at room temperature for at least two hours, with agitation to encourage self-assembly with the Nile Red. After this incubation period, fluorescence is measured using a BioTek Microplate Reader with emission collected from 580-720 nm. Through plate reader data, the linear fits of a max intensity vs log concentration plot are taken and set equal to one another to solve for the critical aggregation concentration represented by the x value of the equations.

2.6 DPPH Assay

A 500 μM stock of DPPH (~1 mg/5.07 mL) was prepared and diluted to 100 μM in methanol and stored in the dark at -20 °C. Samples of, E_3 (5 mM), glutathione antioxidant (200 mM), and glutathione PA (10 mM), were diluted down to working concentrations for the assay (0, 0.125, 0.25, 0.5, 1, 1.5, 2, 2.5, 3 mM) and prepared at 200 μL each.

In a 96 well plate, 50 μL of DPPH and 50 μL of each of the 7 respective samples were plated in triplicate in addition to a water blank. Once each sample was plated, the plate was lightly rocked back and forth for mixture and incubated at room temperature in the dark for 30 minutes. After incubation, the plate was read at an absorbance of 517 nm in a BioTek plate reader. Data workup included subtracting the water blank value from each of the wells. The average of the 0 mM samples which reflects the DPPH absorbance alone, was then used as the divisor of each sample. The resulting quotient of each concentration was averaged and plotted in a normalized intensity vs. concentration graph.

2.7 *In Vitro* Assays

Human embryonic kidney cells (HEK293) were grown to 90% confluence in tissue culture polystyrene flasks in an incubator held at 37 °C and 5% CO_2. Cells were in Dulbecco's Modified Eagle Medium (DMEM) media supplemented with 10% fetal bovine serum (FBS) and 1% penicillin-streptomycin. Trypsin was added to dissociate cells and they were collected into a falcon tube and centrifuged at 5000 RPM for 5 minutes. Briefly, HEK293 cells were resuspended in DMEM media supplemented with 10% FBS and 1% penicillin-streptomycin and cells were counted using the Invitrogen Countess 3 Automated Cell Counter. HEK cells were seeded in a 96 well plate at a volume of 100 μL. Cells were left to adhere overnight and compounds were then

incubated for 24 hours to determine cytotoxicity. The plate contained control wells for spontaneous LDH activity and maximum LDH. At 24 hours, 10 μL of maximum lysis buffer was added to max LDH wells of the main plate and set to react for 45 minutes. Following the 45-minute reaction period, 50 μL of all wells from the starting plate were placed into a new 96 well plate. In this new plate, 50 μL of reaction mixture were pipetted into all wells and allowed to incubate at room temperature, in the dark for 30 minutes. After incubation, 50 μL of stop solution are added to the wells. Throughout the process, care is taken to not introduce bubbles when pipette, as they can affect the absorbance readings. The plate was read at 480 & 680 nm on a microplate reader. The background readings were subtracted to calculate both the average and % cytotoxicity.

CHAPTER III: RESULTS AND DISCUSSION

3.1 Solid Phase Peptide Synthesis

The synthesis of the antioxidant PA was successfully achieved through SPPS using the Fmoc process. Characterization of the synthesized antioxidant PA was performed using MALDI-TOF mass spectrometry and ESI-MS **(Figure 5)**. MALDI-TOF MS analysis confirmed the expected molecular weights of the synthesized PA at 1442.649 g/mol, validating the successful synthesis and accurate molecular composition of the peptide sequences. The observed mass peaks corresponded to the protonated molecular ions [M + H]+, confirming successful synthesis of the antioxidant PA.

Furthermore, ESI-MS analysis was conducted following purification of the peptide amphiphile. The ESI-MS spectra exhibited similar mass peaks confirming the accuracy and reproducibility of the MALDI-TOF MS findings. The absence of additional peaks or impurities in the ESI-MS spectra further confirmed the composition and homogeneity of the synthesized antioxidant PAs.

Overall, the successful synthesis and characterization of antioxidant PAs through MALDI-TOF MS and ESI-MS demonstrate the effectiveness of SPPS in producing peptide-based biomaterials with precise molecular control and high purity. The accurate synthesis of the antioxidant PA allowed for the further study of antioxidant and self-assembling properties which indicated an ideal start to this body of work.

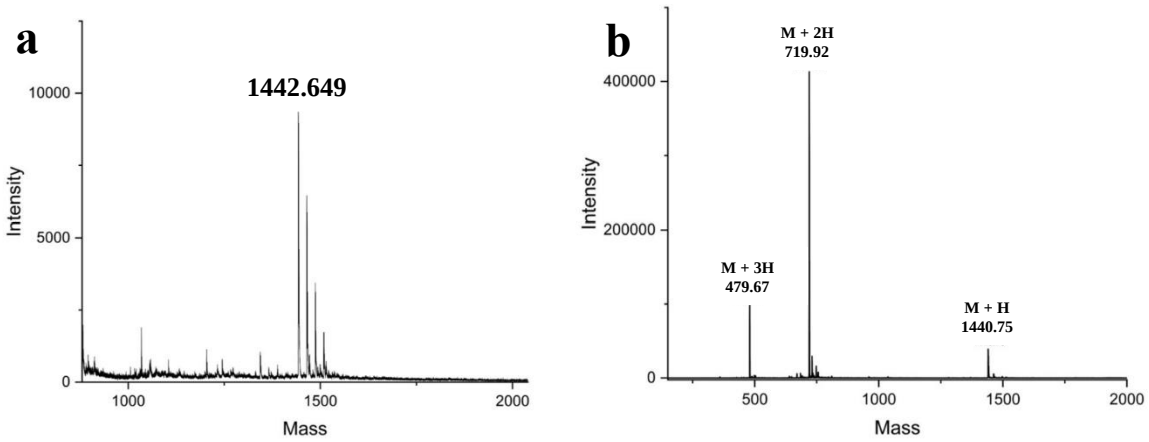

Figure 5. *a)MALDI-TOF data highlighting spectra of crude in support of successful synthesis of antioxidant PA. b)ESI-MS data following purification of the PA highlighting isolation of the compound of interest.*

3.2 Transmission Electron Microscopy

TEM was implemented to view the morphology and nanostructure of the PAs. Images as shown in **Figure 6** revealed the formation of well-defined nanostructures highlighting the self-assembly capabilities of the PAs. The presence of uniformity among fiber length further indicates the amphiphilic nature of the supramolecular assemblies. The observed nanofiber morphology is consistent with the characteristic assembly pattern of peptide amphiphiles, wherein the hydrophobic segments of the peptide sequences aggregate to form the core of the nanofibers, while the hydrophilic segments extend outward, providing solubility and stability in aqueous environments. As designed, the diluent PA serve as the positive control for fiber formation and show longer fiber lengths. The presence of the antioxidant sequence, while allowing fiber formation, has an effect on the self-assembly process and nanostructure formation. As expected, there are

noticeable differences in fiber density, size, and organization between the two PAs. Despite these variations, the formation of fibers in the antioxidant PA indicates success in the synthesis to potentially exhibit the desired properties of biomedical applications. These one-dimensional nanofibers entangle to create a three-dimensional network of entangled fibers capable of acting as a tissue scaffold.

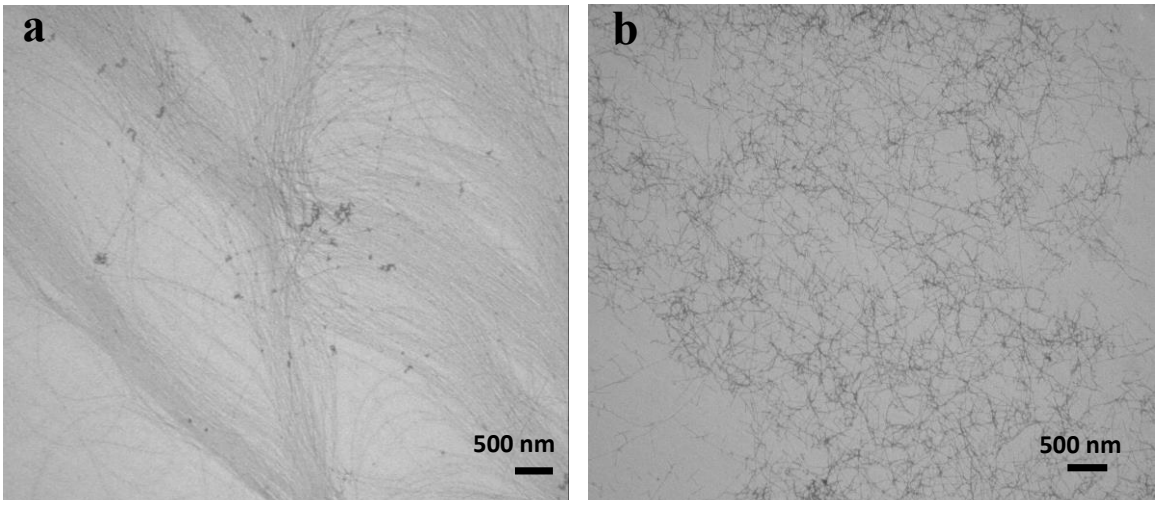

Figure 6. *a) TEM image of Diluent PA. b) TEM image of antioxidant PA**.** Scale bar at 500 nm.*

3.3 Circular Dichroism

Circular Dichroism spectroscopy was employed to confirm the secondary structure of the diluent PA and antioxidant PA and is shown at a concentration of 250 μM **(Figure 7)**. Both PAs exhibited characteristic CD spectra with prominent features in the beta sheet region, indicative of significant beta sheet secondary structure content. The CD spectra of both diluent and antioxidant PAs displayed negative ellipticity in the range of 218 nm, consistent with the signature of beta sheet structures. This observation suggests

that both types of PAs adopt beta sheet-rich conformations, which are stabilized by hydrogen bonding interactions.

Although both diluent and antioxidant PAs exhibited beta sheet-rich secondary structures, significant differences in the CD spectra were observed between the two samples. The intensity and shape of the CD signals in the beta sheet region varied. At 195 nm, the diluent PA had a maximum at ~250 $M^{-1}cm^{-1}$ while the antioxidant PA demonstrated a maximum at ~50 $M^{-1}cm^{-1}$. These differences may arise from variations in the molecular composition or self-assembly behavior induced by the presence of antioxidant functionalities in the peptide sequence. Additionally, both PAs demonstrate the characteristic minima at 218 nm, however, a broadening of the minima may be attributed to the conformational flexibility allowed due to the presence of the antioxidant group. Ultimately, the presence of the beta sheet region signifies the ideal synthesis of the antioxidant PA and the maintenance of secondary structure in the assembled state.

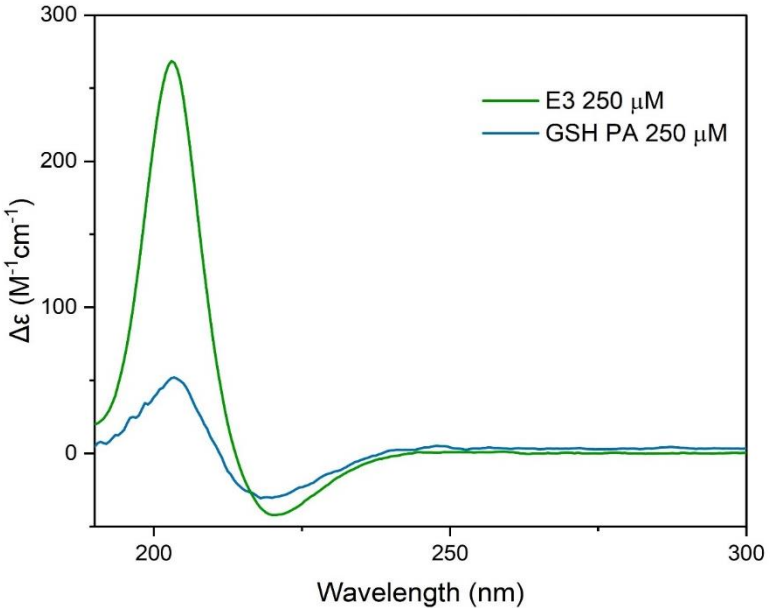

Figure 7. *Circular dichroism spectra for the diluent PA and*

3.4 Nile Red Assay

The critical aggregation concentration (CAC) was determined via a Nile Red assay, providing insights into the concentration at which the supramolecular polymerization process begins. The fluorescent intensity of Nile Red was measured at varying concentrations of PA at 0, 1, 0.1, 1, 2, 5, 10, 20, 25, 50, 100, 250, and 500 μM, which were plotted to show the aggregation of the amphiphilic molecules. The onset of appreciable Nile red fluorescence is indicative of the concentration at which the hydrophobic interactions of the amphiphilic molecules supports aggregation and the supramolecular formation of fibers occurs. The comparison of the spectral scans of the three molecules exhibited favorable results in self-assembly trends. As expected, the E_3 and GSH PA both exemplified fiber formation at ~8 μM which is consistent with previous studies conducted in our lab with PAs. The negative control of the antioxidant GSH does not demonstrate any interaction with Nile red across the concentrations examined, indicative of no hydrophobic core assembly from the peptide alone **(Figure 8c)**. The analysis completed through the Nile Red assay provides support to the hypothesis made regarding the antioxidant PA showing positive fiber formation as glutathione is proven to be successfully coupled to a peptide sequence with the property to sufficiently form nanofibers. The characterization of the supramolecular polymerization of GSH PA through the Nile Red assay establishes a foundation for understanding the structural properties of the peptide synthesis and their potential utility in addressing the harmful effects of ROS.

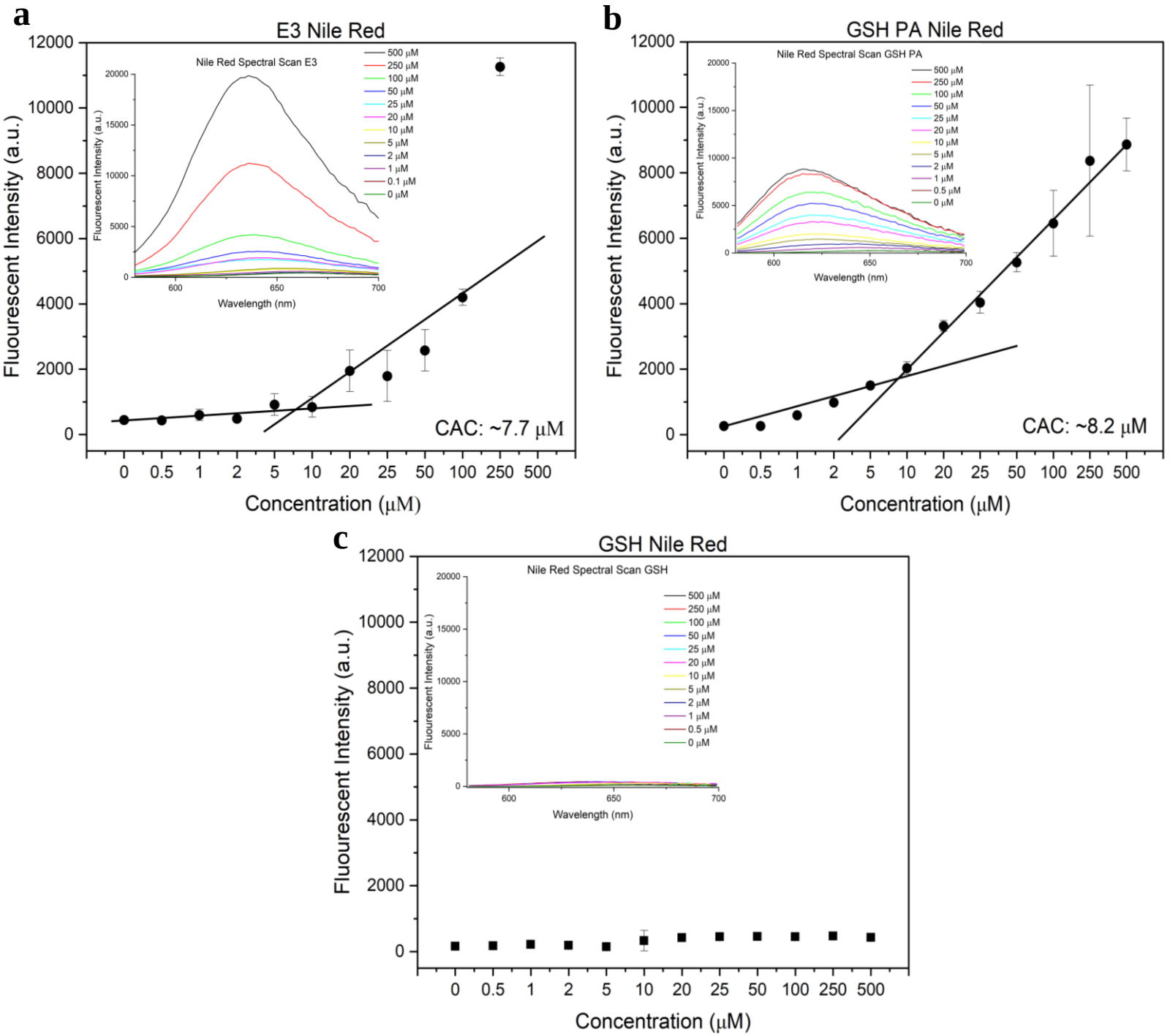

Figure 8. *CAC data and spectral scans at varying concentrations represented for a) Diluent PA, b) GSH PA, c) GSH antioxidant*

3.5 DPPH Assay

The quenching capabilities of the selected molecules were assessed using a 2,2-diphenyl-1-picrylhidrazyl (DPPH) assay. The normalized intensity was measured at 517 nm across concentrations of 0, 0.125, 0.25, 0.5, 1, 1.5, 2, 2.5, and 3 mM. The assay is based on the reduction of the stable DPPH radical in the presence of antioxidants. For this assay, the antioxidant presence results directly in the reduction of the normalized intensity. As the negative control, E_3 exhibited no antioxidant capabilities, as hypothesized. This is represented in the graph by a straight line at high normalized intensity. The positive control, GSH antioxidant, properly exhibited significant antioxidant capabilities as the normalized intensity decreased as concentration of treatment increased. The GSH PA also exhibited antioxidant properties reflecting the successful synthesis as it contains the intended properties of free radical scavenging. The free thiol of GSH was maintained through synthesis and purification. It is suspected that confining GSH to the fibers slightly reduced its antioxidant capabilities in the assay compared to the free GSH because of the steric hindrance of the bulky DPPH radical. Furthermore, GSH's mechanism of action depends on disulfide bridges forming between two molecules. When tethered to the fiber, GSH may be chemically reduced as they cannot readily diffuse.

However, the obtained results demonstrate the ability of the PA supramolecular polymers to effectively scavenge DPPH radicals, indicating their antioxidant properties. This assay provides quantitative data on the scavenging capacity of the synthesized peptides and antioxidant, supporting their potential application as therapeutic agents for combating oxidative damage. The promising outcomes of this DPPH assay contribute to

the overall evidence supporting the feasibility of antioxidant supramolecular polymers as a novel approach for addressing the damaging effects of reactive oxygen species in cardiovascular diseases.

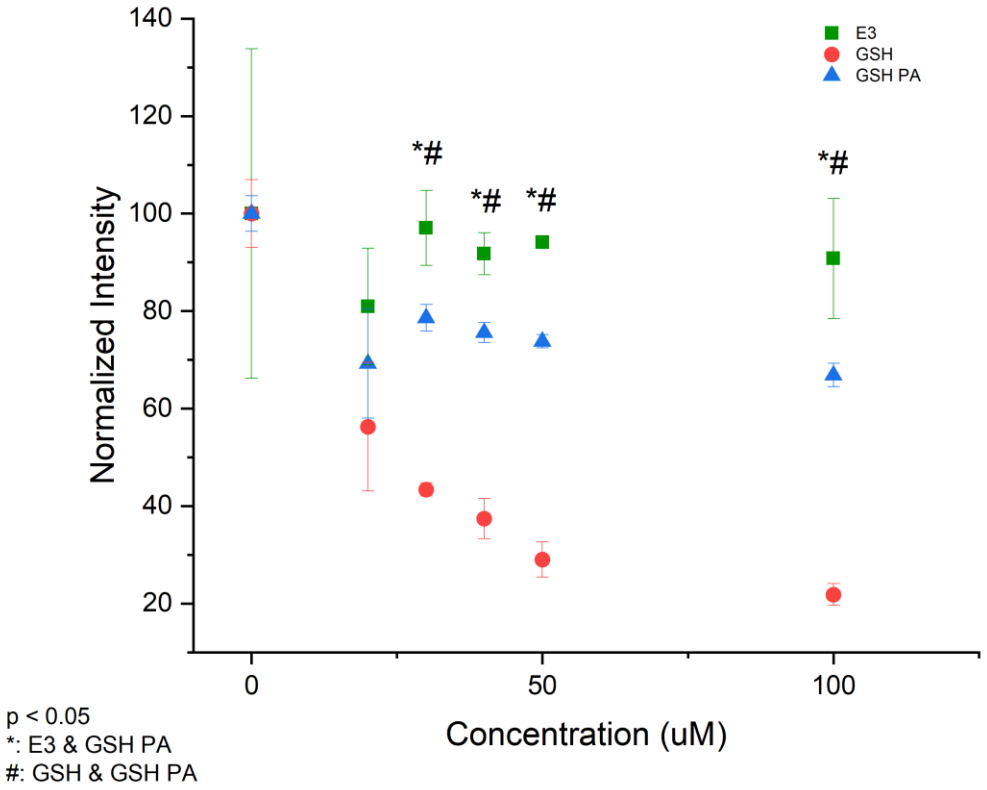

Figure 9. *Quenching measured at varying concentrations to reflect antioxidant activity.*

3.6 *In Vitro* Assays

The use of *in vitro* assays was implemented to begin to understand the bioactive capabilities of the PAs. The results from this work included the initial cytotoxicity study, the employment of a cell agonist to simulate ROS release, and the ability of the PAs to perform cell rescue. The completion of these assays indicated the potential for the

antioxidant PA to be further expounded upon in study as it performed well as a novel material.

3.6.1 Initial Cytotoxicity

To probe the biocompatibility of the designed PAs, the diluent PA and antioxidant PA were interacted with cells with no additional added conditions. The results demonstrated minimal cytotoxic effects of both diluent and antioxidant PAs across a range of concentrations. Specifically, cell viability remained high (>80%) even at the highest tested concentration of PAs indicating ideal biocompatibility of the synthesized materials. These findings are consistent with previous studies reporting low cytotoxicity of peptide amphiphiles, which can be attributed to their biocompatible peptide backbone and absence of toxic chemical residues.

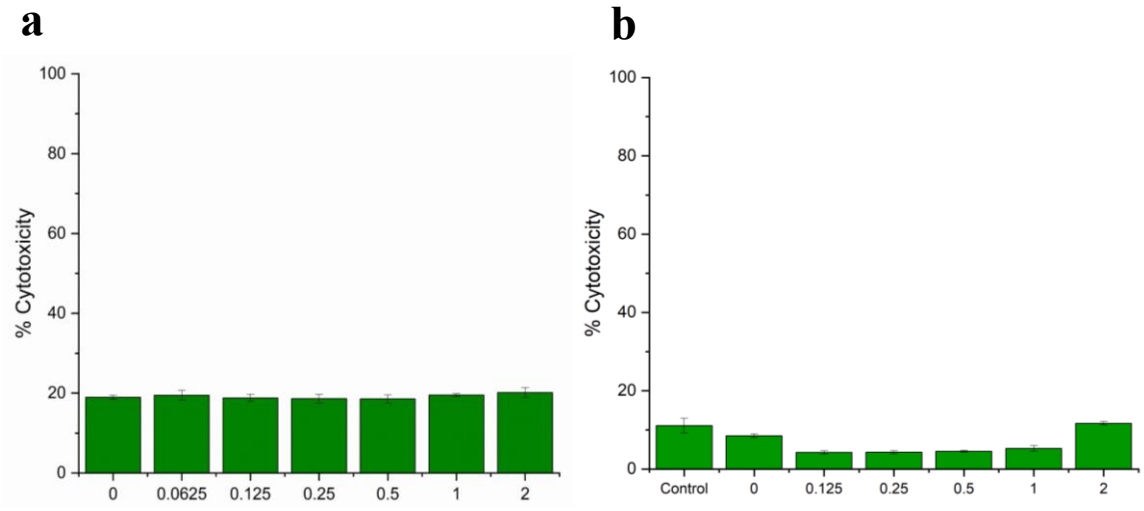

Figure 10. *a) 24 hour Cytotoxicity results of diluent PA. b) 24 hour Cytotoxicity results of antioxidant* PA

3.6.2 TBHP as Agonist

As one of the potential cell agonists, the compound tert-butyl hydroperoxide (TBHP) was implemented to induce ROS production within cells leading to ROS release and cell death. TBHP acts by interrupting intracellular glutathione cascades and disrupting the natural antioxidant balance intracellularly. Thus, it was applied into a set of cells to determine its cytotoxicity within HEK 293 cells. The assessment of TBHP revealed high cytotoxicity profiles, consistent with its role as a potent agonist for ROS release. By inducing ROS production, TBHP mimics the oxidative stress conditions associated with various pathological conditions, such as cardiovascular disease, neurodegenerative disorders, and cancer.

The results demonstrated dose-dependent cytotoxic effects of TBHP on the treated cells, with significant reductions in cell viability observed at concentrations as low as 10 μM. At concentrations above 25 μM, the cytotoxicity had no significant increase showing that a concentration of 30 μM is plausible for a system to assess the therapeutic capabilities of the PAs. The goal was to determine a point where cell death was generated by ROS escaping to the extracellular environment and killing other cells, a process known as secondary degeneration. At concentrations above 100 uM catastrophic cell death was caused, leading to exclusion from this study. If all cells are dying from the ROS agonist, there is no chance to rescue cells from damaging extracellular ROS. These findings are consistent with the known cytotoxic properties of TBHP, which acts as a strong oxidizing agent and generates ROS through lipid peroxidation and oxidative stress mechanisms.

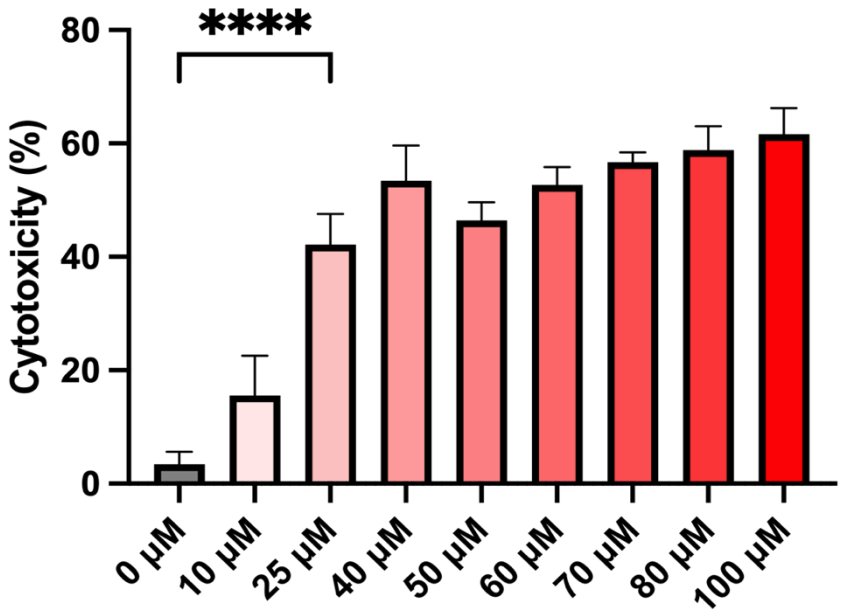

Figure 11. *Cytotoxicity results of TBHP compound ranging from 0 to 100.*

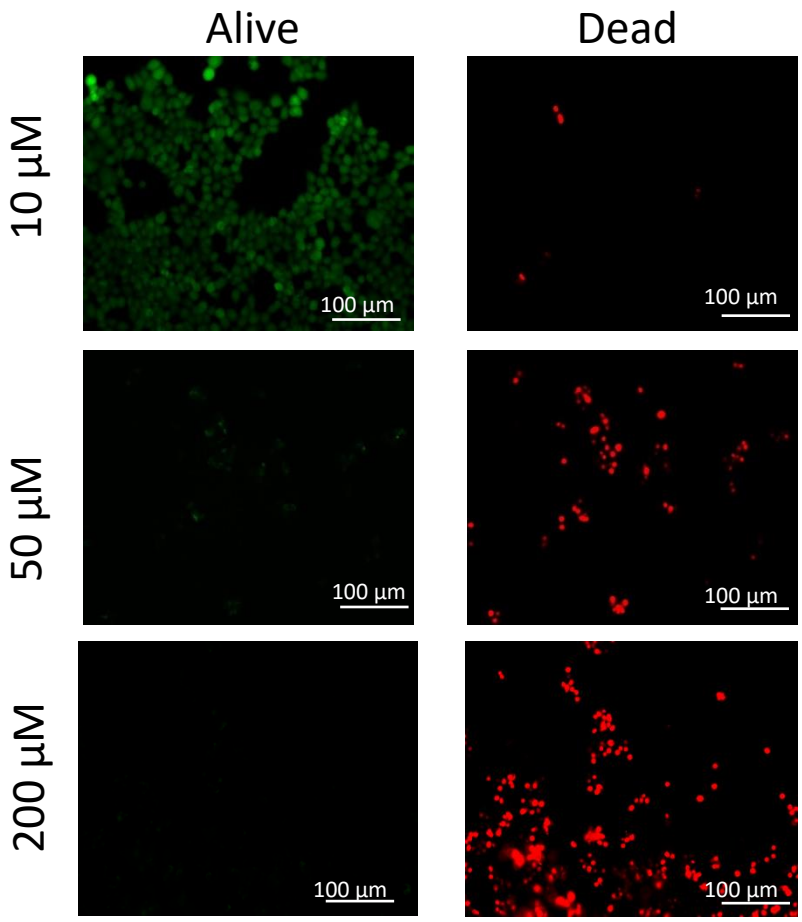

Figure 12. *LIVE/DEAD cell images from TBHP implementation showing effects of agonist.*

3.6.3 Cell Rescue

The cytotoxicity studies conducted with TBHP treatment demonstrated that significant cell death could be induced. TBHP was then incubated with both diluent and antioxidant PAs at varying PA concentrations to determine to protective effects of the PA. Cells were left for 24 hours and analyzed though LDH Assay and Live/Dead imaging. It was seen that the antioxidant PA exhibited cell rescue effects, mitigating the cytotoxic effects induced by ROS-mediated oxidative stress more than the diluent PA

control. Unfortunately, large statistical error on these measurements and low sample numbers prevented there from being statistical significance, despite qualitative observations that GSH PA outperforms the diluent PA control at all concentrations. Cell viability assays using LDH release as an indicator of cytotoxicity were performed on cultured cells treated with TBHP in the presence or absence of the diluent and antioxidant PA. As lower concentrations were studied, the results are particularly evident in the LIVE/DEAD images seen in **Figure 13**. By scavenging ROS and preventing oxidative damage to cellular components, the antioxidant PA preserved cell viability and protected against the cytotoxic effects induced by TBHP-mediated oxidative stress. Further experiments are needed to confirm this effect, as the expected level of cell death from TBHP was not achieved in this experiment, however, this work provides an exciting basis for extracellular ROS capture for cell rescue.

Moreover, the cell rescue effects of antioxidant PAs highlight their potential as therapeutic agents for mitigating oxidative stress-related diseases and injuries. By modulating cellular responses to oxidative stress, antioxidant PAs offer a promising strategy for preserving tissue function and promoting tissue regeneration in various pathological conditions characterized by ROS-mediated damage.

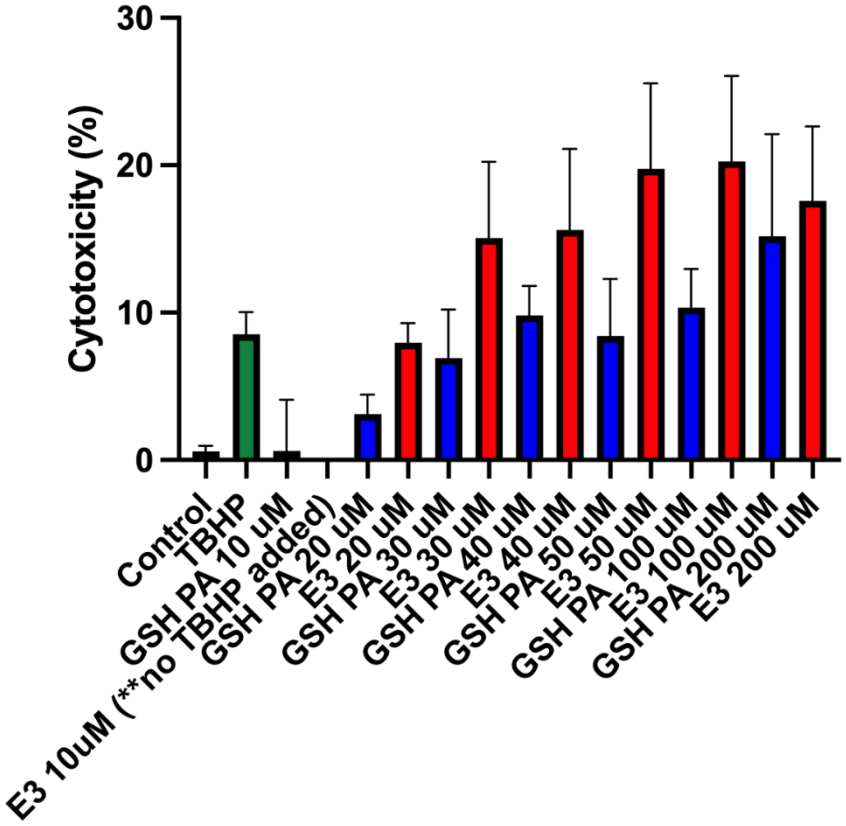

Figure 13. *Cytotoxicity results of PAs with TBHP irritation simulated in cells.*

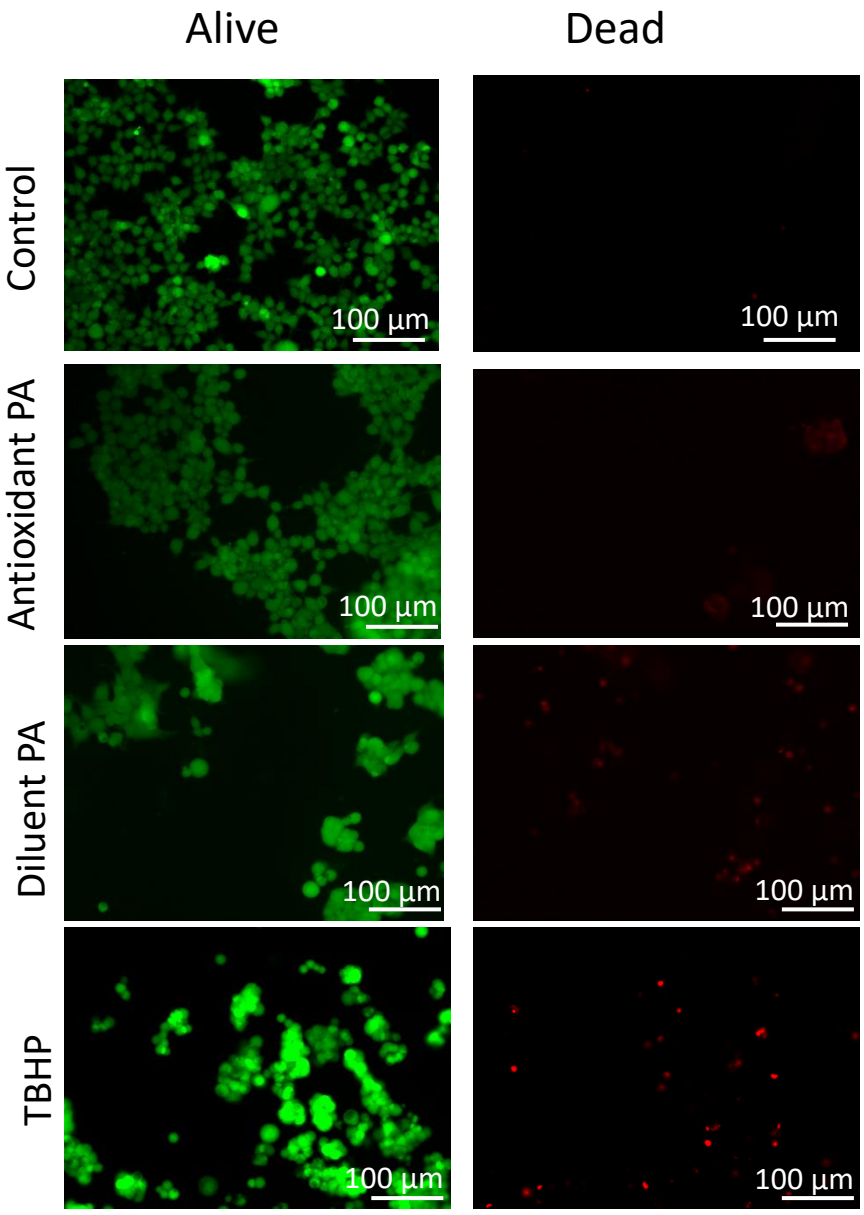

Figure 14. *LIVE/DEAD cell images from PA and TBHP implementation.*

CHAPTER IV: CONCLUSION

The high prevalence of CVD and other pathologies hallmarked by a sharp increase in ROS identify the need for therapies that can suppress these damaging effects. As discussed, the application of supramolecular polymers can be implemented to provide this therapeutic effect. This study marks a significant advancement in the synthesis and characterization of antioxidant PAs offering promising prospects for addressing the substantial societal impact of oxidative stress-related disorders. The accurate characterization of the synthesized PAs through MALDI-TOF MS and ESI-MS underscores the precision and reliability of the synthesis process, laying the foundation for their potential therapeutic application. As compared to a diluent PA and the glutathione antioxidant, the antioxidant PA successfully maintained fiber forming capabilities as well as its antioxidant activity. The Nile Red, DPPH, and *in vitro* assays combined provided a holistic foundation to studying the potential for therapies by use of PAs. Specifically, the addition of TBHP and the cell rescue seen in the antioxidant PA provides starting success for fiber formation, antioxidant activity, and bioactivity.

Future work would incorporate comprehensive preclinical studies to evaluate the efficacy and safety of the antioxidant PA in animal models of oxidative stress-related diseases. These studies would provide valuable insights into the therapeutic potential of antioxidant PAs, paving the way for translational research and clinical trials in human subjects.

Furthermore, the incorporation of other antioxidants, such as natural or synthetic compounds, into the peptide sequences of the PA could enhance their ROS scavenging capabilities and broaden their therapeutic applications. By combining multiple

antioxidants with complementary mechanisms of action, novel antioxidant PAs with enhanced efficacy and specificity could be developed for targeted interventions in oxidative stress-related disorders.

Overall, continued research efforts in this field are essential to translate the promising findings of antioxidant PAs into clinical solutions for suppression of the damaging effects of ROS. The outcome of this work provides evidence that there is high potential for the implication of our novel material to be a therapeutic route at treating CVD and other pathologies. By advancing our understanding of the therapeutic potential of antioxidant PAs and optimizing their design and delivery strategies, we can harness the power of antioxidants to combat oxidative stress and improve patient outcomes in diverse clinical settings.

REFERENCES

(1) World Health Organization. *Cardiovascular Diseases (CVDs)*. 2021. https://www.who.int/news-room/fact-sheets/detail/cardiovascular-diseases-(cvds)
(2) World Health Federation. https://world-heart-federation.org/news/deaths-from-cardiovascular-disease-surged-60-globally-over-the-last-30-years-report/
(3) Kreatsoulas, C.; Anand, S. S. The impact of social determinants on cardiovascular disease. *Can J Cardiol* **2010**, *26 Suppl C* (Suppl C), 8C-13C. DOI: 10.1016/s0828-282x(10)71075-8.
(4) Adams, D. J.; Boskovic, Z. V.; Theriault, J. R.; Wang, A. J.; Stern, A. M.; Wagner, B. K.; Shamji, A. F.; Schreiber, S. L. Discovery of small-molecule enhancers of reactive oxygen species that are nontoxic or cause genotype-selective cell death. *ACS Chem Biol* **2013**, *8* (5), 923-929. DOI: 10.1021/cb300653v.
(5) Ye, H.; Zhou, Y.; Liu, X.; Chen, Y.; Duan, S.; Zhu, R.; Liu, Y.; Yin, L. Recent Advances on Reactive Oxygen Species-Responsive Delivery and Diagnosis System. *Biomacromolecules* **2019**, *20* (7), 2441-2463. DOI: 10.1021/acs.biomac.9b00628.
(6) Szeto, H. H. Mitochondria-targeted peptide antioxidants: novel neuroprotective agents. *AAPS J* **2006**, *8* (3), E521-531. DOI: 10.1208/aapsj080362.
(7) Bao, F.; Liu, D. Hydroxyl radicals generated in the rat spinal cord at the level produced by impact injury induce cell death by necrosis and apoptosis: protection by a metalloporphyrin. *Neuroscience* **2004**, *126* (2), 285-295. DOI: 10.1016/j.neuroscience.2004.03.054.
(8) Dubois-Deruy, E.; Peugnet, V.; Turkieh, A.; Pinet, F. Oxidative Stress in Cardiovascular Diseases. *Antioxidants (Basel)* **2020**, *9* (9). DOI: 10.3390/antiox9090864.
(9) Cadenas, S. ROS and redox signaling in myocardial ischemia-reperfusion injury and cardioprotection. *Free Radic Biol Med* **2018**, *117*, 76-89. DOI: 10.1016/j.freeradbiomed.2018.01.024.
(10) Solaini, G.; Harris, D. A. Biochemical dysfunction in heart mitochondria exposed to ischaemia and reperfusion. *Biochem J* **2005**, *390* (Pt 2), 377-394. DOI: 10.1042/BJ20042006.
(11) Garcia-Dorado, D.; Rodriguez-Sinovas, A.; Ruiz-Meana, M.; Inserte, J.; Agulló, L.; Cabestrero, A. The end-effectors of preconditioning protection against myocardial cell death secondary to ischemia-reperfusion. *Cardiovasc Res* **2006**, *70* (2), 274-285. DOI: 10.1016/j.cardiores.2006.02.011.
(12) Wang, W.; Kang, P. M. Oxidative Stress and Antioxidant Treatments in Cardiovascular Diseases. *Antioxidants (Basel)* **2020**, *9* (12). DOI: 10.3390/antiox9121292.
(13) Rodrigo, R.; Fernández-Gajardo, R.; Gutiérrez, R.; Matamala, J. M.; Carrasco, R.; Miranda-Merchak, A.; Feuerhake, W. Oxidative stress and pathophysiology of ischemic stroke: novel therapeutic opportunities. *CNS Neurol Disord Drug Targets* **2013**, *12* (5), 698-714. DOI: 10.2174/18715273113120500015.
(14) Yellon, D. M.; Hausenloy, D. J. Myocardial reperfusion injury. *N Engl J Med* **2007**, *357* (11), 1121-1135. DOI: 10.1056/NEJMra071667.
(15) Clemons, T. D.; Stupp, S. I. Design of materials with supramolecular polymers. *Prog Polym Sci* **2020**, *111*, 101310. DOI: 10.1016/j.progpolymsci.2020.101310.

(16) Cui, H.; Webber, M. J.; Stupp, S. I. Self-assembly of peptide amphiphiles: from molecules to nanostructures to biomaterials. *Biopolymers* **2010**, *94* (1), 1-18. DOI: 10.1002/bip.21328.
(17) Webber, M. J.; Tongers, J.; Newcomb, C. J.; Marquardt, K. T.; Bauersachs, J.; Losordo, D. W.; Stupp, S. I. Supramolecular nanostructures that mimic VEGF as a strategy for ischemic tissue repair. *Proc Natl Acad Sci U S A* **2011**, *108* (33), 13438-13443. DOI: 10.1073/pnas.1016546108.
(18) Du, Z.; Fan, B.; Dai, Q.; Wang, L.; Guo, J.; Ye, Z.; Cui, N.; Chen, J.; Tan, K.; Li, R.; et al. Supramolecular peptide nanostructures: Self-assembly and biomedical applications. *Giant* **2022**, *9*, 100082. DOI: https://doi.org/10.1016/j.giant.2021.100082.
(19) Lu, S. C. Glutathione synthesis. *Biochim Biophys Acta* **2013**, *1830* (5), 3143-3153. DOI: 10.1016/j.bbagen.2012.09.008.
(20) Ballatori, N.; Krance, S. M.; Notenboom, S.; Shi, S.; Tieu, K.; Hammond, C. L. Glutathione dysregulation and the etiology and progression of human diseases. *Biol Chem* **2009**, *390* (3), 191-214. DOI: 10.1515/BC.2009.033.
(21) Gaucher, C.; Boudier, A.; Bonetti, J.; Clarot, I.; Leroy, P.; Parent, M. Glutathione: Antioxidant Properties Dedicated to Nanotechnologies. *Antioxidants (Basel)* **2018**, *7* (5). DOI: 10.3390/antiox7050062.
(22) Stawikowski, M.; Fields, G. B. Introduction to peptide synthesis. *Curr Protoc Protein Sci* **2012**, *Chapter 18*, 18.11.11-18.11.13. DOI: 10.1002/0471140864.ps1801s69.
(23) *Solid Phase Peptide Synthesis (SPPS) Explained*. BACHEM, 2023. https://www.bachem.com/news/solid-phase-peptide-synthesis-explained/
(24) *Liberty Blue 2.0*. CEM, 2022. https://cem.com/liberty-blue-2#.
(25) *What is HPLC?* SHIMADZU, 2022. https://www.shimadzu.com/an/service-support/technical-support/analysis-basics/basic/what_is_hplc.html#3
(26) *Prodigy*. CEM, 2022. https://cem.com/prodigy
(27) Ho, C. S.; Lam, C. W.; Chan, M. H.; Cheung, R. C.; Law, L. K.; Lit, L. C.; Ng, K. F.; Suen, M. W.; Tai, H. L. Electrospray ionisation mass spectrometry: principles and clinical applications. *Clin Biochem Rev* **2003**, *24* (1), 3-12.
(28) *Electrospray Ionization*. Creative Proteomics, 2022. https://www.creative-proteomics.com/support/electrospray-ionization.htm
(29) *Transmission Electron Microscopy*. NanoScience Instruments, 2023. https://www.nanoscience.com/techniques/transmission-electron-microscopy/
(30) *LVEM25 Electron Microscope*. Delong Instruments, 2017. https://delongamerica.com//lvem25/product-details
(31) Andrews, S. S.; Tretton, J. Physical Principles of Circular Dichroism. *Journal of Chemical Education* **2020**, *97* (12), 4370-4376. DOI: 10.1021/acs.jchemed.0c01061.
(32) Kedare, S. B.; Singh, R. P. Genesis and development of DPPH method of antioxidant assay. *J Food Sci Technol* **2011**, *48* (4), 412-422. DOI: 10.1007/s13197-011-0251-1.